Available online at www.sciencedirect.com
SCIENCE DIRECT
Journal of Electrostatics 64 (2006) 29–34
Journal of ELECTROSTATICS
www.elsevier.com/locate/elstat

The electrostatic capacitance of an inclined plate capacitor

Yumin Xiang

Department of Basic Sciences, Sichuan University of Science and Engineering, Sichuan 643033, China

Received 31 December 2003; received in revised form 22 December 2004; accepted 12 May 2005
Available online 28 June 2005

Abstract

Considering the dimension and relative position of the two plates, the capacitance of an inclined plate capacitor is precisely calculated. Conformal mappings are employed and elliptic functions are used for achieving the general result. Taking the fringing effect into account, the inner capacitance and outer capacitance of the inclined angle are added to obtain a reliable result. The expression for computing the fringing capacitance of a parallel-plate capacitor and the capacitance of a parallel-strip transmission line in a plane are presented as special cases.

Keywords: Inclined plate capacitor; Conformal mapping; Elliptic function; Inner capacitance; Outer capacitance

1. Introduction

The capacitor is an important type of electrical element used extensively in engineering. One common type is a parallel-plate capacitor consisting of two conducting plates parallel to each other. The latter is a key element in Micro Electromechanical Systems [1,2] because the electrostatic capacitance can be controlled with precision. However, due to manufacturing and application constraints, one electrode plate is often inclined and not parallel to the other. The objective of this paper is to determine the capacitance of two inclined plates in the general case, where the fringing effect is considered and the geometric dimensions of the two plates are not necessarily the same. The parallel-plate capacitor, treated only as the limit's case, is also discussed. An immediate related application of the general result is for calculating the capacitance between two parallel strip transmission lines in a plane.

2. Field region transformation

The capacitor considered in this paper consists of two non-parallel conducting plates of sufficient longitudinal length. Its cross section in the z-plane is shown in Fig. 1. The extended lines of the two plates intersect at the origin O. The length of the plates are $AB = l_1$ and $CD = l_2$, respectively, and the indicated distances are $OA = r_1$ and $OC = r_2$. The angle between the plates is $\angle AOC = \varphi$. A voltage V is applied across the two electrode plates. The sufficient longitudinal dimension of the plates guarantees that the problem can be regarded as two-dimensional in the cross-section plane.

The electrostatic field in the z-plane contains two parts. One is confined by two electrode plates to the interior of the angle $\angle AOC$ and another exists outside the angle. Attention is focused first on the former. That region can be mapped onto the upper half of the t-plane of Fig. 2. Since the corresponding angle $\angle AOC$ is equal to π in the t-plane, the conformal mapping should be as follows [3]:

$$t = M z^{\pi/\varphi} + M_0. \tag{1}$$

E-mail address: xiangyumin@tom.com.

0304-3886/$ - see front matter
doi:10.1016/j.elstat.2005.05.002

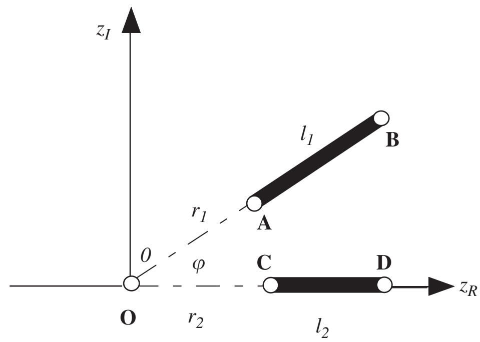

Fig. 1. The cross-section of an inclined plate capacitor in the z-plane.

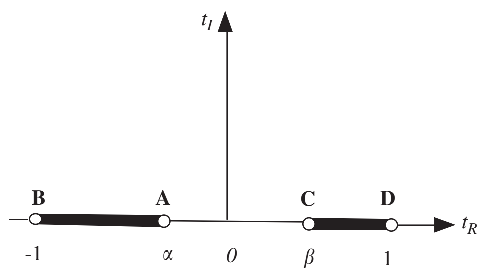

Fig. 2. The t-plane.

The coordinate B in the z-plane is $z=(r_1+l_1)\mathrm{e}^{j\varphi}$; it becomes $t=-1$ in the t-plane. The coordinate of point D in the z-plane is $z=r_2+l_2$, while in the t-plane it is $t=1$. Substituting these values into Eq. (1), we obtain

$$M=\frac{2}{(r_1+l_1)^{\pi/\varphi}+(r_2+l_2)^{\pi/\varphi}}$$

and

$$M_0=\frac{(r_1+l_1)^{\pi/\varphi}-(r_2+l_2)^{\pi/\varphi}}{(r_1+l_1)^{\pi/\varphi}+(r_2+l_2)^{\pi/\varphi}}. \tag{2}$$

Eq. (1) can then be rewritten as

$$t=\frac{2z^{\pi/\varphi}+(r_1+l_1)^{\pi/\varphi}-(r_2+l_2)^{\pi/\varphi}}{(r_1+l_1)^{\pi/\varphi}+(r_2+l_2)^{\pi/\varphi}}. \tag{3}$$

We next use the coordinates of point A in those two planes: $z=r_1\mathrm{e}^{j\varphi}$ and $t=\alpha$, where from Eq. (3) we have

$$\alpha=\frac{-2r_1^{\pi/\varphi}+(r_1+l_1)^{\pi/\varphi}-(r_2+l_2)^{\pi/\varphi}}{(r_1+l_1)^{\pi/\varphi}+(r_2+l_2)^{\pi/\varphi}}. \tag{4}$$

Similarly, the coordinate of point C in the t-plane is found from the equation

$$\beta=\frac{2r_2^{\pi/\varphi}+(r_1+l_1)^{\pi/\varphi}-(r_2+l_2)^{\pi/\varphi}}{(r_1+l_1)^{\pi/\varphi}+(r_2+l_2)^{\pi/\varphi}}. \tag{5}$$

Further, employing following fractional linear transformation:

$$\zeta=\frac{(1-\alpha)(1+t)}{2(t-\alpha)}, \tag{6}$$

the field region in the t-plane can be mapped into the ζ-plane of Fig. 3 in order to calculate the modulus k_{in} conveniently.

Substituting $t=\beta$ and $\zeta=1/k_{\text{in}}^2$ at point C into Eq. (6), the modulus k_{in} is given by

$$\begin{aligned}k_{\text{in}}&=\sqrt{\frac{2(\beta-\alpha)}{(1-\alpha)(1+\beta)}}\\&=\sqrt{\frac{\left(r_1^{\pi/\varphi}+r_2^{\pi/\varphi}\right)\left((r_1+l_1)^{\pi/\varphi}+(r_2+l_2)^{\pi/\varphi}\right)}{\left(r_1^{\pi/\varphi}+(r_2+l_2)^{\pi/\varphi}\right)\left(r_2^{\pi/\varphi}+(r_1+l_1)^{\pi/\varphi}\right)}}.\end{aligned} \tag{7}$$

Fig. 4 shows the upper half of ζ-plane mapped into the interior of the rectangle ABDC in the u-plane by the Schwarz–Crystoffel transformation

$$\frac{\mathrm{d}u}{\mathrm{d}\zeta}=N\zeta^{1/2}(\zeta-1)^{1/2}\left(\zeta-\frac{1}{k_{\text{in}}^2}\right)^{1/2}. \tag{8}$$

Integration of Eq. (8) leads to

$$u=k_{\text{in}}N\int_0^{\zeta}\frac{\mathrm{d}\zeta}{\sqrt{\zeta(1-\zeta)(1-k^2\zeta)}}+N_0. \tag{9}$$

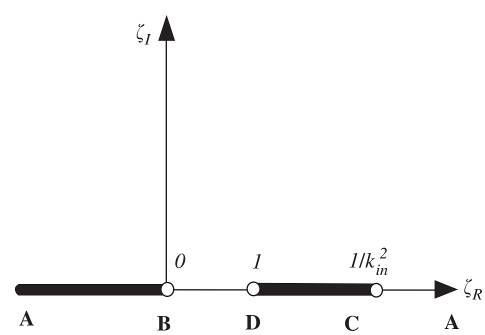

Fig. 3. The ζ-plane.

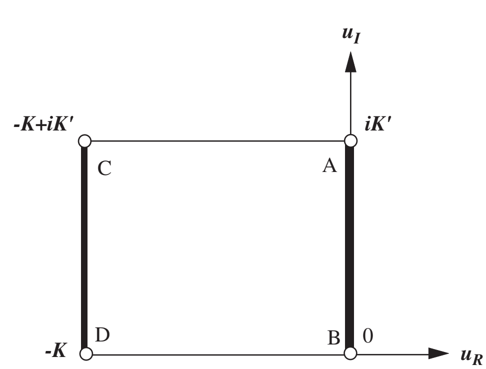

Fig. 4. The u-plane.

Letting $\zeta = \rho^2$, Eq. (9) then becomes

$$\begin{aligned} u &= 2k_{\text{in}}N\int_0^{\rho}\frac{\mathrm{d}\rho}{\sqrt{(1-\rho^2)(1-k_{\text{in}}^2\rho^2)}}+N_0 \\ &= N_1\int_0^{\rho}\frac{\mathrm{d}\rho}{\sqrt{(1-\rho^2)(1-k_{\text{in}}^2\rho^2)}}+N_0 \\ &= N_1F(\rho,k_{\text{in}})+N_0, \end{aligned} \tag{10}$$

where $F(\rho, k)$ is the incomplete elliptic integration of the first kind. Based on the definition of the Jacobian elliptic function $sn(v, k)$ [4], the foregoing equation is replaced by

$$\rho = sn\left(\frac{u-N_0}{N_1}, k_{\text{in}}\right) \quad \text{and} \quad \zeta = sn^2\left(\frac{u-N_0}{N_1}, k_{\text{in}}\right). \tag{11}$$

Substitution of $u = 0$ as $\zeta = 0$ at B and $u = -K(k_{\text{in}})$ as $\zeta = 1$ at D into Eq. (11) gives

$$N_0 = 0 \quad \text{and} \quad N_1 = 1, \tag{12}$$

where $K(k)$ is the complete elliptic integral of the first kind. Consequently, the second one of Eq. (11) reduces to

$$\zeta = sn^2(u,\ k_{\text{in}}). \tag{13}$$

Resorting to the conformal transformations, a field region with a simple rectangular boundary is obtained in the u-plane.

3. Electrostatic capacitance

The field bounded by the rectangle ABDC in the u-plane is uniform [5]. Therefore, the inner capacitance of the region inside $\angle AOC$ per unit longitudinal length of the plate is

$$C_{\text{in}} = \varepsilon_0\frac{K'(k_{\text{in}})}{K(k_{\text{in}})}, \tag{14}$$

where

$$K'(k) = K(k') \tag{15}$$

and k' indicates the complementary modulus of k, i.e.

$$\begin{aligned} k'_{\text{in}} &= \sqrt{\frac{(1+\alpha)(1-\beta)}{(1-\alpha)(1+\beta)}} \\ &= \sqrt{\frac{\left((r_1+l_1)^{\pi/\varphi}-r_1^{\pi/\varphi}\right)\left((r_2+l_2)^{\pi/\varphi}-r_2^{\pi/\varphi}\right)}{\left((r_1+l_1)^{\pi/\varphi}+r_2^{\pi/\varphi}\right)\left((r_2+l_2)^{\pi/\varphi}+r_1^{\pi/\varphi}\right)}}. \end{aligned} \tag{16}$$

For the field region outside of the angle $\angle AOC$, using $2\pi - \varphi$ instead of φ in Eqs. (7), (14) and (16), we obtain the outer capacitance of the region outside $\angle AOC$ per unit longitudinal length

$$C_{\text{out}} = \varepsilon_0\frac{K'(k_{\text{out}})}{K(k_{\text{out}})}, \tag{17}$$

where

$$k_{\text{out}} = \sqrt{\frac{\left(r_1^{\pi/2\pi-\varphi}+r_2^{\pi/2\pi-\varphi}\right)\left((r_1+l_1)^{\pi/2\pi-\varphi}+(r_2+l_2)^{\pi/2\pi-\varphi}\right)}{\left(r_1^{\pi/2\pi-\varphi}+(r_2+l_2)^{\pi/2\pi-\varphi}\right)\left(r_2^{\pi/2\pi-\varphi}+(r_1+l_1)^{\pi/2\pi-\varphi}\right)}} \tag{18}$$

and

$$k'_{\text{out}} = \sqrt{\frac{\left((r_1+l_1)^{\pi/2\pi-\varphi}-r_1^{\pi/2\pi-\varphi}\right)\left((r_2+l_2)^{\pi/2\pi-\varphi}-r_2^{\pi/2\pi-\varphi}\right)}{\left((r_1+l_1)^{\pi/2\pi-\varphi}+r_2^{\pi/2\pi-\varphi}\right)\left((r_2+l_2)^{\pi/2\pi-\varphi}+r_1^{\pi/2\pi-\varphi}\right)}}. \tag{19}$$

Therefore, the electrostatic capacitance per unit longitudinal length can be computed by

$$C = C_{\text{in}} + C_{\text{out}} = \varepsilon_0\left(\frac{K'(k_{\text{in}})}{K(k_{\text{in}})}+\frac{K'(k_{\text{out}})}{K(k_{\text{out}})}\right). \tag{20}$$

4. Further discussion

For convenience, the parameters h_1 and δ_1 are introduced to replace r_1 and r_2. As sketched in Fig. 5, h_1 is the distances from A toCD and $\delta_1 = \angle ACZ_R$. The following geometric relations apply:

$$\begin{aligned} &h_2 = h_1 + l_1\ \sin\ \varphi, \quad \cot\ \delta_2 = \frac{h_1\ \cot\ \delta_1 + l_1\ \cos\ \varphi - l_2}{h_1 + l_1\ \sin\ \varphi}, \\ &r_1 = \frac{h_1}{\sin\ \varphi}, \quad r_2 = \frac{h_1\ \sin(\delta_1-\varphi)}{\sin\ \varphi\ \sin\ \delta_1}, \\ &r_1 + l_1 = \frac{h_2}{\sin\ \varphi}, \quad r_2 + l_2 = \frac{h_2\ \sin(\delta_2-\varphi)}{\sin\ \varphi\ \sin\ \delta_2}. \end{aligned} \tag{21}$$

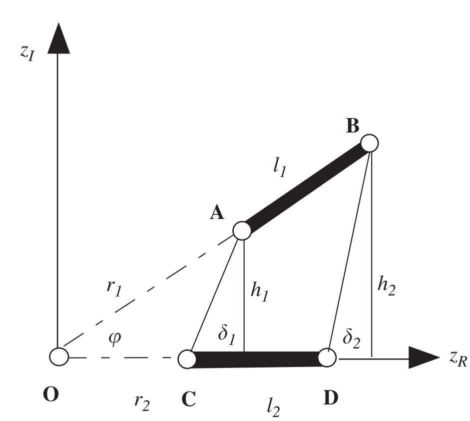

Fig. 5. Geometric relation of the lines and angles in the z-plane.

Substituting Eq. (21) into Eq. (7) leads to

$$k_{\text{in}} = \sqrt{\frac{\left(1+\left(\frac{\sin(\delta_1-\varphi)}{\sin\delta_1}\right)^{\pi/\varphi}\right)\left(1+\left(\frac{\sin(\delta_2-\varphi)}{\sin\delta_2}\right)^{\pi/\varphi}\right)}{\left(1+\left(\frac{(h_1+l_1\sin\varphi)\sin(\delta_2-\varphi)}{h_1\sin\delta_2}\right)^{\pi/\varphi}\right)\left(1+\left(\frac{h_1\sin(\delta_1-\varphi)}{(h_1+l_1\sin\varphi)\sin\delta_1}\right)^{\pi/\varphi}\right)}}. \tag{22}$$

Likewise, replacing φ with $2\pi-\varphi$ in Eq. (22) yields

$$k_{\text{out}} = \sqrt{\frac{\left(1+\left(\frac{\sin(\delta_1+\varphi)}{\sin\delta_1}\right)^{\pi/2\pi-\varphi}\right)\left(1+\left(\frac{\sin(\delta_2+\varphi)}{\sin\delta_2}\right)^{\pi/2\pi-\varphi}\right)}{\left(1+\left(\frac{(h_1-l_1\sin\varphi)\sin(\delta_2-\varphi)}{h_1\sin\delta_2}\right)^{\pi/2\pi-\varphi}\right)\left(1+\left(\frac{h_1\sin(\delta_1+\varphi)}{(h_1-l_1\sin\varphi)\sin\delta_1}\right)^{\pi/2\pi-\varphi}\right)}}. \tag{23}$$

5. Parallel-plate capacitor

The parallel-plate capacitor is a special case obtained as φ approaches zero. Note that

$$\lim_{\varphi\to 0}\left(\sin(\delta-\varphi)/\sin\delta\right)^{\pi/\varphi} = \exp(-\pi\cot\delta) \quad \text{and}$$
$$\lim_{\varphi\to 0}(1+m\sin\varphi)^{\pi/\varphi} = \exp(m\pi). \tag{24}$$

As $\varphi\to 0$ from Eqs. (21) and (22) we have

$$h_2 = h_1 = h, \quad \cot\delta_2 = \cot\delta_1 + \frac{l_1-l_2}{h} \tag{25}$$

and

$$k_{\text{in}} = \sqrt{\frac{(1+\exp(-\pi\cot\delta_1))(1+\exp(-\pi\cot\delta_2))}{\left(1+\exp\left(-\pi\left(\frac{l_1}{h}+\cot\delta_1\right)\right)\right)\left(1+\exp\left(\pi\left(\frac{l_2}{h}-\cot\delta_1\right)\right)\right)}}. \tag{26}$$

Utilizing $\varphi\to 0$ in Eq. (23) leads to

$$k_{\text{out}} = 1. \tag{27}$$

Then Eq. (17) yields

$$C_{\text{out}} = 0. \tag{28}$$

A typical case for the parallel-plate capacitor is that $l_1 = l_2 = l$ and $\delta_1 = \pi/2$. Hence, from Eq. (25) we obtain

$$\delta_2 = \frac{\pi}{2}. \tag{29}$$

Eq. (26) then reduces to

$$k_{\text{in}} = \operatorname{sech}\pi\frac{l}{2h}. \tag{30}$$

Substituting Eqs. (30) and (28) into Eq. (20), we obtain the capacitance in this case:

$$C = \varepsilon_0\frac{K'\left(\operatorname{sech}\pi\frac{l}{2h}\right)}{K\left(\operatorname{sech}\pi\frac{l}{2h}\right)}. \tag{31}$$

It will be seen that an explicit expression for Eq. (31) can also be obtained. Note that

$$\frac{K'(k_{\text{in}})}{K(k_{\text{in}})} = -\frac{1}{\pi}\ln q. \tag{32}$$

We may also introduce

$$\lambda = \frac{1-\sqrt{k'_{\text{in}}}}{2(1+\sqrt{k'_{\text{in}}})}. \tag{33}$$

From the computation of the complete elliptic integration, we have

$$\lambda = \frac{\vartheta_3+\vartheta_4}{2(\vartheta_3+\vartheta_4)} = \frac{q+q^5+q^{25}+\cdots}{1+2q^4+2q^{16}+2q^{35}+\cdots}, \tag{34}$$

where ϑ represents the ϑ-function [6]. The solution of the above equation for q is

$$q = \lambda + 2\lambda^5 + 15\lambda^9 + 150\lambda^{35} + \cdots \tag{35}$$

Eq. (33) implies that $\lambda<1/2$ because $0<k'_{\rm in} = \tanh[\pi l/2h]<1$. The power series on the left side of Eq. (35) converges very quickly. Combining Eqs. (31), (32) and (35), one arrives at

$$C = -\frac{\varepsilon_0}{\pi}\left[\ln\lambda + \ln(1+2\lambda^4+15\lambda^8+150\lambda^{34}+\cdots)\right]. \tag{36}$$

Taking the logarithm of Eq. (33) leads to

$$\begin{aligned}\ln\lambda &= \ln\frac{1-\sqrt{k'}}{2(1+\sqrt{k'})} \\ &= \ln\frac{1-\sqrt{\tanh\frac{\pi l}{2h}}}{2\left(1+\sqrt{\tanh\frac{\pi l}{2h}}\right)} \\ &= -\frac{\pi l}{h} - \ln 2\left(1+\sqrt{1-\exp\left(-\frac{\pi l}{2h}\right)}\right).\end{aligned} \tag{37}$$

Substituting Eq. (37) into Eq. (36) we obtain

$$\begin{aligned}C = \frac{\varepsilon_0 l}{h} + \frac{\varepsilon_0}{\pi}\Bigg[&\ln 2\left(1+\sqrt{1+\exp\left(-\frac{\pi l}{2h}\right)}\right) \\ &- \ln(1+2\lambda^4+15\lambda^8+150\lambda^{34}+\cdots)\Bigg].\end{aligned} \tag{38}$$

It is immediately clear that the fringing capacitance [7] can then be expressed as

$$\begin{aligned}C_{\rm f} = \frac{\varepsilon_0}{\pi}\Bigg[&\ln 2\left(1+\sqrt{1+\exp\left(-\frac{\pi l}{2h}\right)}\right) \\ &- \ln(1+2\lambda^4+15\lambda^8+150\lambda^{34}+\cdots)\Bigg].\end{aligned} \tag{39}$$

For the purpose of computing precise capacitance values numerically, the series can be truncated on the right side of the two above equations. Under the condition $\lambda \ll 1$, and as long as $l \gg h$ from Eqs. (30) and (33), taking the first several items of the series is sufficient. Moreover, from Eq. (38) we approximately have

$$C = \varepsilon_0\frac{1}{h} \tag{40}$$

which is commonly used to describe the capacitance of a parallel-plate capacitor.

6. Parallel-strip transmission line

Referring to Fig. 6, the capacitance per unit longitudinal length of a transmission line formed by two parallel strips in a plane [8] can be derived directly

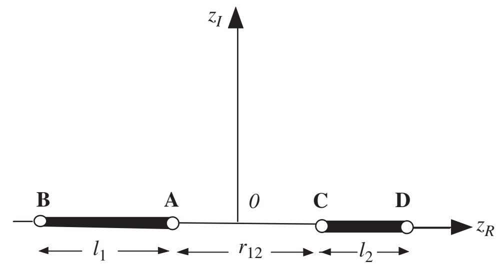

Fig. 6. The cross-section of a parallel-strip transmission line in a plane.

from the general result in Section 3. Letting $\varphi = \pi$, from Eqs. (7) and (18) we can derive the result

$$k_{\rm in} = k_{\rm out} = k_{//} = \sqrt{\frac{r_{12}(r_{12}+l_1+l_2)}{(r_{12}+l_1)(r_{12}+l_2)}}, \tag{41}$$

where r_{12} is the distance between the two strips:

$$r_{12} = r_1 + r_2. \tag{42}$$

Hence, using Eq. (20), the capacitance per unit longitudinal length of the line is

$$C = C_{\rm in} + C_{\rm out} = 2\varepsilon_0\frac{K'(k_{//})}{K(k_{//})}. \tag{43}$$

7. Conclusion

Inclined plate capacitor represents a more general case than parallel-plate capacitor for the ones used in engineering. Precisely calculating the capacitance of an inclined plate capacitor has significance for theoretical analysis and engineering practice. The diverse plate dimension, the various relative position of the plates, and fringing effect increase the complexity of the calculation. However, the conformal mapping method, with the aid of elliptic functions, provides a concise way of solving the problem in which both the inner and outer capacitances are considered. The parallel-plate capacitor becomes simply a special case as the inclined angle approaches zero. Based on the general expression for the capacitance of a parallel-plate capacitor, the fringing capacitance can be computed numerically by computer with high precision. The capacitance of a transmission line comprised of two parallel strips in a plane is an immediate corollary of the general result.

Acknowledgements

This research is supported by the Education Commission of Sichuan Province of China.

References

[1] A.J.C. Luo, F.Y. Wang, Nonlinear dynamics of a micro-electro-mechanical system with time-varying capacitors, J. Vib. Acoust. 1 (2004) 77–83.

[2] A.J.C. Luo, F.Y. Wang, Chaotic motion in a micro-electro-mechanical system with non-linearity from capacitors, Commun. Nonlinear Sci. Numer. Simulation 7 (2002) 31–49.

[3] S. Lang, Complex Analysis, second ed., Springer, New York, 1985.

[4] D.V. Patric, Elliptic Functions and Elliptic Curves, Cambridge, London, 1973.

[5] Y. Xiang, W. Lin, A study of electrostatic force on the walls of N-regular polygon-multifin line, J. Electrostat. 50 (2001) 119–128.

[6] A.G. Greenhill, The Application of Elliptic Functions, Dover, New York, 1959.

[7] C. Shen, J.K. Kong, Applied Electromagnetism, PWS Engineering, New York, 1987.

[8] Y. Xiang, Electrostatic force between two parallel strip transmission lines in a plane, J. Univ. Electron. Sci. Technol. China 29 (1) (2000) 45–48.